Journal of Cellular Biochemistry 95:1012–1028 (2005)

Major Contribution of the Multidrug Transporter P-Glycoprotein to Reduced Susceptibility of Poly(ADP-Ribose) Polymerase-1 Knock-Out Cells to Doxorubicin Action

Józefa Węsierska-Gądek*

Department of Medicine I, Cell Cycle Regulation Group, Institute of Cancer Research, Medical University of Vienna, Vienna, Austria

Abstract Inactivation of poly(ADP-ribose) polymerase-1 (PARP-1) has been shown to potentiate the cytotoxicity of distinct DNA targeting agents including topoisomerase I inhibitors. On the other hand, the PARP-1 deficient cells exhibited resistance to conventional inhibitors of topoisomerase II such as etoposide or doxorubicin (DOX). Recently, we observed the extreme sensitivity of PARP-1 knock-out (KO) cells to C-1305, a new biologically active triazoloacridone compound. C-1305 permanently arrested the cells in G_2-phase of the cell-cycle. These observations prompted us to investigate more thoroughly the susceptibility of PARP-1 KO cells to DOX and to examine the effect of DOX on the progression of cell-cycle. We determined the uptake of DOX and P-glycoprotein (P-gp) expression in mouse cells and compared it with that in human myeloma 8226/Dox40 cells overexpressing P-gp. Exposure of mouse cells to DOX revealed a reduced drug uptake in cells lacking PARP-1. However, combined treatment with verapamil, a potent MDR modulator increased the DOX accumulation. Detailed immunoblotting experiments revealed an approximately threefold higher P-gp level in PARP-1 KO cells as compared with normal counterparts. Interestingly, DOX induced in normal fibroblasts very rapidly G_2 arrest whereas in PARP-1 KO cells it blocked primarily the transition between S and G_2 resulting in the increase of cells remaining in S-phase. This coincided with the lack of the site-specific phosphorylation of CDK2. Simultaneous inhibition of P-gp in cells lacking PARP-1 resulted in an accumulation of cells in G_2. Exposure of mouse cells to high DOX dose activated significantly caspase-3/7 in PARP-1 KO cells. J. Cell. Biochem. 95: 1012–1028, 2005.

Key words: cell-cycle arrest; G_2 accumulation; MDR1; p53 activation; multidrug resistance; apoptosis; caspases-3/7 activation; CDKs activity; site-specific phosphorylation; doxorubicin uptake

Poly(ADP-ribose) polymerase-1 (PARP-1), known for a long time as the only one enzyme capable of catalyzing covalent attachment of multiple ADP-ribose molecules to a variety of acceptor proteins, became recently a member of a growing multigene family (for review, see [D'Amours et al., 1999; Ame et al., 2004]). Despite the similarity of catalytic activity between the members of the gene family, only PARP-1 possesses zinc finger motifs responsible for recognition of damaged DNA and binding to DNA strand breaks. PARP-1, which is highly expressed in the nucleus, responds very rapidly to DNA damage and facilitates DNA repair. Once activated, PARP-1 cleaves nicotinamide adenine dinucleotide (NAD^+) and transfers up to 200 ADP-ribose residues to target proteins

Abbreviations used: CDK, cyclin dependent kinase; DOX, doxorubicin; KO, knock-out; MDR, multidrug resistance; MEFs, mouse embronic fibroblasts; PARP-1, poly(ADP-ribose) polymerase-1; PD, petri dish; P-gp, P-glycoprotein; PM, plasma membrane; PVDF, polyvinylidene difluoride; VP-16, etoposide; WCL, whole cell lysate; WT, wild-type.

Grant sponsor: Jubiäumsfonds of the Oesterreichische Nationalbank; Grant number: 10364.

*Correspondence to: Józefa Węsierska-Gądek, Cell Cycle Regulation Group, Institute of Cancer Research, Medical University of Vienna, Borschkegasse 8 a, A-1090 Vienna, Austria.

E-mail: Jozefa.Gadek-Wesierski@meduniwien.ac.at

Received 29 December 2004; Accepted 2 February 2005

DOI 10.1002/jcb.20467

thereby consuming the cellular NAD^+ reserve. It seems that massive PARP-1 activation contributes to a major part to depletion of cellular NAD^+ and ATP, ultimately leading to energy failure and cell death. The finding that PARP-1 suppression by chemical inhibitors or by inactivation of the *PARP-1* gene could prevent cell death evoked the great interest on the poly-(ADP-ribosyl)ation reactions. The most important observation was that inhibition of PARP-1 activity could protect against diabetes, ischemia, inflammation, and septic shock [Szabo and Dawson, 1998].

On the other hand, suppression of PARP-1 activity has been shown to potentiate the cytotoxicity of distinct DNA targeting agents including topoisomerase I inhibitors [Delaney et al., 2000; Calabrese et al., 2004]. In contrast to the hypersensitivity to drugs targeting topoisomerase I, the PARP-1 activity depleted cells exhibited resistance to conventional inhibitors of topoisomerase II such as etoposide or doxorubicin (DOX) [Chatterjee et al., 1995; Wurzer et al., 2000]. The resistance of PARP-1 depleted cells to etoposide was attributable to induction of grp78 protein [Chatterjee et al., 1995]. On the other hand, the reduced susceptibility of PARP-1 knock-out (KO) cells to DOX coincided with an increase in the expression of multidrug resistance (MDR) transporter protein P-glycoprotein (P-gp) [Wurzer et al., 2000]. Recently, we observed the extreme sensitivity of PARP-1 KO cells to C-1305, a new topoisomerase II inhibitor [Wesierska-Gadek et al., 2004]. C-1305 is a novel, biologically active triazoloacridone compound that selectively inhibits topoisomerase II β [Lemke et al., 2004]. C-1305 strongly inhibited the proliferation of PARP-$1^{-/-}$ mouse fibroblasts and permanently arrested the cells in G_2-phase of the cell-cycle [Wesierska-Gadek et al., 2004]. These findings prompted us to investigate more thoroughly the susceptibility of PARP-1 KO cells to DOX and to examine its effect on the progression of cell-cycle. We determined the uptake of DOX and P-gp expression in mouse cells and compared it with that in human myeloma 8226/Dox40 cells known to overexpress P-gp protein. Mouse cells lacking PARP-1 accumulated only low amounts of DOX that coincided with about threefold higher expression of P-gp as compared with normal counterparts. The combined treatment with verapamil, a MDR modulator, highly increased intracellular accumulation of DOX. Exposure of normal mouse cells to DOX resulted in a rapid accumulation of G_2-arrested cells. However, treatment of cells lacking PARP-1 with DOX resulted in a block of the transition between S and G_2 associated with an increase of the cell number remaining in S-phase. The combined treatment of mutant cells with verapamil resulted in an increase of the frequency of G_2 population. The increased accumulation of DOX treated PARP-1 KO cells in S-phase coincided with the lack of site-specific phosphorylation of CDK2 that is a prerequisite for its activation. Interestingly, exposure of mouse cells to high DOX concentration markedly activated caspases-3/7 in PARP-$1^{-/-}$ cells. Addition of the MDR reversor enhanced significantly the activation of caspases.

Our results confirm previous observations that inactivation of PARP-1 reduced the basal level of wt p53 protein and cellular p53 response to DOX what coincided with an increase of P-gp expression [Wurzer et al., 2000].

MATERIALS AND METHODS

Cells

Mice lacking PARP-1 were generated by homologous recombination [Wang et al., 1995]. Immortalized MEFs were obtained from PARP-$1^{+/+}$ (A-19) and from PARP-$1^{-/-}$ (A-11 and A-12) mice. Cells were grown in DMEM supplemented with 10% (v/v) FCS at 37°C in an atmosphere of 8% CO_2. Human 8226 myeloma cells obtained from the American Type Culture Collection (Rockville, MD) were selected for resistance to DOX by gradually increasing DOX exposure over a 2-year period [Dalton et al., 1986]. The 8226/DOX_{40} cells were gradually exposed to a maximum concentration of 4×10^{-7} M DOX, representing a 40-fold increase in the initial drug exposure concentration [Dalton et al., 1986]. Cells were maintained as a suspension in RPMI 1640 medium supplemented with 10% (v/v) FCS at 37°C in a 5% CO_2–95% air atmosphere [Dalton et al., 1986, 1989]. Human cervix carcinoma HTB-31 cells and human breast carcinoma MCF-7 cells were used in some experiments as positive controls and were maintained as described earlier [Wojciechowski et al., 2003].

Drugs and Chemicals

Doxorubicin hydrochloride was purchased from Calbiochem-Novabiochem, (La Jolla, CA).

Verapamil hydrochloride and probenecid were obtained from Sigma Co. (St. Louis, MO).

Cell Treatment

Cells were treated for the indicated periods of time with the anti-cancer drug DOX at concentrations ranging from 0.05–5 μM alone or in combination with MDR modulators [verapamil (10 μM) and probenecid (1 mg/ml)]. MDR modulators were added 1 h before DOX administration.

Antibodies

We used the following antibodies: monoclonal anti-p53 antibodies PAb421 (Ab-1) directed against an epitope within the carboxy-terminus of the mouse protein, monoclonal anti-p53 antibodies DO-1 and DO-7 recognizing epitopes within the amino-terminus of human protein. Human monoclonal anti-PARP-1 antibodies (C-2-10) and monoclonal anti-MCM7 (clone DCS141.2) were from Oncogene Research Products (Cambridge, MA). Polyclonal anti-NF-κB p65 (C-20) was from Santa Cruz Biotechnology, (Santa Cruz, CA). Monoclonal anti-MDR1 C219 antibody was from Fujirebio Diagnostics, Inc. (Tokyo, Japan) and JSB-1 antibody was from Monosan (Uden, the Netherlands). Polyclonal antibodies against phospho-CDK1 (Thr161), phospho-CDK2 (Thr160), and monoclonal anti-phospho-cdc25C phosphatase (Ser216) antibodies (clone 9D1) were from Cell Signaling Technology, Inc. (Beverly, MA). Polyclonal antibodies against phospho-CDK1 (Thr14/Tyr15) and monoclonal anti-α-tubulin antibody (Clone B-5-1-2) were from Sigma Co. Antibodies against CDK1 and cdc25C phosphatase (clone TC-15) were from Upstate Biotechnology (Lake Placid, NY). Monoclonal anti-CDK2 antibodies (2B6 + 8D4) were from NeoMarkers, Inc. (Fremont, CA). Monoclonal anti-actin (Clone C4) antibodies were from ICN Biochemicals (Aurora, OH). The secondary antibodies were purchased from Upstate Biotechnology.

DOX Uptake

Cells were incubated with DOX at a final concentration of 0.2 and 2 μM with or without 10 μM verapamil for 12 and 24 h at 37°C. After termination of the treatment adherent cells were detached by treatment with trypsin or accutase [Wesierska-Gadek et al., 2004]. Collected cells were washed four times with PBS, counted, and resuspended in PBS (1×10^6 cells per standard tube). Intracellular accumulation of DOX was immediately measured using FL3 in a FACScan cytometer (Becton Dickinson).

MDR1 Shift Assay

To detect active MDR1, we performed a MDR1 shift assay (Chemicon International, Temecula, CA) according to the manufacturer's protocol. The human 8226/DOX_{40} cells were used as a reference cell line expressing MDR1 [Dalton et al., 1986, 1989]. The MDR1 shift assay provides a convenient method to detect conformational changes in MDR1 that occurs upon transport of MDR1 substrates. Binding of UIC2 was analyzed by flow cytometry using FL2 for indirect UIC2 staining and FL3 for propidium iodide to exclude dead cells. At least 10,000 events were collected.

Analysis of DNA Content in Cells by Flow Cytometry

The measurement of DNA content in propidium iodide-stained nuclei was performed by flow cytometry as described previously [Vindelov et al., 1983; Wesierska-Gadek and Schmid, 2000]. The stained cells were analyzed using a FACScan cytometer. Distribution of cells in distinct cell-cycle phases was determined using ModFIT cell-cycle analysis software. DNA histograms were obtained by CellQuest evaluation program.

Determination of Caspase-3/7 Activity

The activity of both caspases was determined using the APO-ONE Homogenous Caspase-3/7 Assay (Promega, Madison, WI) which uses the caspase-3/7 substrate rhodamine 110, bis-(*N*-CBZ-L-aspartyl-L-glutamyl-L-valyl-L-aspartic acid amide (Z-DEVD-R100). This compound exists as a pro-fluorescent substrate prior to the assay. Upon cleavage and removal of the DEVD peptide by caspase-3/7 activity and excitation at 499 nm, the rhodamine 110 leaving group becomes intensely fluorescent.

Mouse cells were plated in 96-wells microtiter plates. Twenty-four hours after plating cells were exposed for 15 h to DOX at concentrations ranging between 0.1 and 4 μM. Thereafter, culture supernatant was transferred into another microtiter plate and the caspases activity was determined separately in cells and in culture medium. Then an equal volume of caspase substrate was added and samples were incubated at 37°C for 2, 4, and 20 h. The fluorescence

was measured at 485 nm. Culture medium was used as a blank. "No-cell background" values after 20 h were about 500 cpm.

Cell Fractionation

Isolation of nuclei was performed according to the method of Capco et al. [1982] as previously described in detail [Wojciechowski et al., 2003]. During all isolation steps, phenylmethylsulfonylfluoride (PMSF) and Pefabloc were added in a final concentration of 1 mM and 50 μM, respectively. Briefly, PBS washed cells were suspended in ice-cold hypotonic buffer, swollen, and were homogenized after addition of detergents (combined ionic and non-ionic detergents). After centrifugation through sucrose cushion nuclei were pelleted. In experiments designed to isolate P-gp enriched fraction, plasma membrane preparations from mouse cells (A-19, A-12, and A-11) and from human 8226/S and 8226/DOX_{40} were purified according to the slightly modified method of Riordan and Ling [Riordan and Ling, 1979].

Determination of Protein Content

Protein concentration in whole cell lysates (WCLs) and in subcellular fractions was determined by the DC assay (Bio-Rad Laboratories, Richmond, CA) using bovine serum albumin (BSA) as a standard.

Electrophoretic Separation of Proteins and Immunoblotting

Total cellular proteins or proteins of the distinct subcellular fractions dissolved in SDS sample buffer were separated on 8%, 10%, or 15% SDS slab gels and transferred electrophoretically onto polyvinylidene difluoride membrane (PVDF) (Amersham International, Little Chalfont, Buckinghamshire, UK). Protein transfer and equal protein loading was confirmed by Ponceau S staining. Blots were incubated with specific primary antibodies at appropriate final dilutions and the immune complexes were detected using corresponding peroxidase-conjugated secondary antibodies and enhanced chemiluminescent detection reagent ECL+ (Amersham International) as described previously [Wesierska-Gadek et al., 2002]. For detection of site-specific phosphorylation of distinct proteins, membranes were processed in Tris-saline buffer [Wesierska-Gadek et al., 2004].

Statistical Analysis

Statistical analysis was performed by the ANOVA test followed by Dunnett's Multiple Comparison Test (all treatment groups versus control).

RESULTS

Reduced DOX Uptake in PARP-1 KO Cells

To assess the intracellular accumulation of DOX, we performed two independent approaches. Both assays were based on the capability of DOX, after entering into cells and binding to DNA, to generate fluorescent signals after excitation with UV light. In the first approach, mouse cells exposed to DOX for 24 h we fixed in situ and cells were analyzed under fluorescence microscopy using a rhodamine filter. As depicted in Figure 1A, PARP-1 deficient mouse cells in contrast to normal counterparts did not accumulate DOX. Even at higher magnification, red fluorescent signals were barely detectable. However, the combined treatment by DOX and verapamil (V), a modulator of MDR, resulted in an elevated accumulation of DOX in PARP-1 KO cells as evidenced by the appearance of the intense red fluorescence. Interestingly, the addition of verapamil had no obvious effect on the intensity of DOX-mediated fluorescence in normal mouse fibroblasts. The analysis of the fluorescence in fixed cells allowed us to determine the DOX accumulation in adherent cells, whereas the floating cells, if any, could not be evaluated. Therefore, in a second approach the intracellular DOX levels were quantified in total cell populations by flow cytometric analysis (Fig. 1B). Exposure of wild-type mouse cells to 0.2 μM DOX resulted in a time- and concentration-dependent accumulation of the drug (Fig. 1B). However, after exposure of PARP-1 deficient cells to DOX for 12 h, the drug entered only about 30% cells, whereas the majority of cells did not accumulate the drug. The combined treatment with verapamil dramatically changed the cellular levels of DOX thereby implicating that reduced drug uptake in the latter is attributable to a higher activity of multidrug transporter proteins. The detailed quantification of DOX uptake is shown in Figure 1C.

Overexpression of P-gp Is Associated With Decreased DOX Accumulation

The exposure of human sensitive and resistant 8226 myeloma cells to 0.2 μM DOX for 6 and

12 h showed the difference in the intracellular accumulation of the drug (Fig. 2A), which correlated with the overexpression of P-gp. The DOX level in 8226/Dox40 cells strongly increased after the combined treatment with verapamil thereby substantiating the assumption that drug resistance of 8226/Dox40 cells is attributable to overexpression of P-gp. The phenotype of 8226/Dox 40 cells resembled that observed in mouse fibroblasts lacking PARP-1.

MDR1 Shift Assay

To detect active MDR1, we performed a MDR1 shift assay (Chemicon) according to the manufacturer's protocol. The binding of antibody UIC_2 to human $8226/DOX_{40}$ cells expressing MDR1 [Dalton et al., 1986, 1989] was determined in the absence and in the presence of vinblastine. As shown in Figure 2B, human resistant 8226/Dox40 cells, in contrast to the sensitive myeloma cell line, were stained by anti-P-gp antibody. The addition of vinblastine, a MDR1 substrate, resulted in conformational changes and an increase of stained cells was observed (Fig. 2B). We also performed the assay on mouse cells. Our preliminary results (not shown) revealed the MDR1 shift in PARP-1 KO cells. However, the total number of positive cells is lower as compared with human 8226/Dox40 cells. These results additionally evidence the functionality of enhanced P-gp in 8226/Dox40 cells.

Increased Expression of P-gp in Mouse Cells Lacking PARP-1

Recently, we compared by immunoblotting using polyclonal antibodies from Santa Cruz the expression P-gp protein between normal and PARP-1 deficient mouse fibroblasts and found higher cellular P-gp level in the latter [Wurzer et al., 2000]. We also isolated the plasma membrane fraction from control and DOX-treated mouse cells and resolved the obtained subcellular fractions on a gel together with a plasma membrane sample from human chemoresistant HL-60 cells used as a P-gp positive control [Wurzer et al., 2000]. Immunoblotting was performed using monoclonal anti-P-gp antibody. The HL-60 plasma membrane sample and an aliquot of anti-P-gp (designed as JSB-1 antibody) was a kind gift of our colleagues Dr. W. Berger and Dr. E. Elbling. As shown in Figure 3A, the antibody detected only a single band at about 170 kDa. The intensity of the

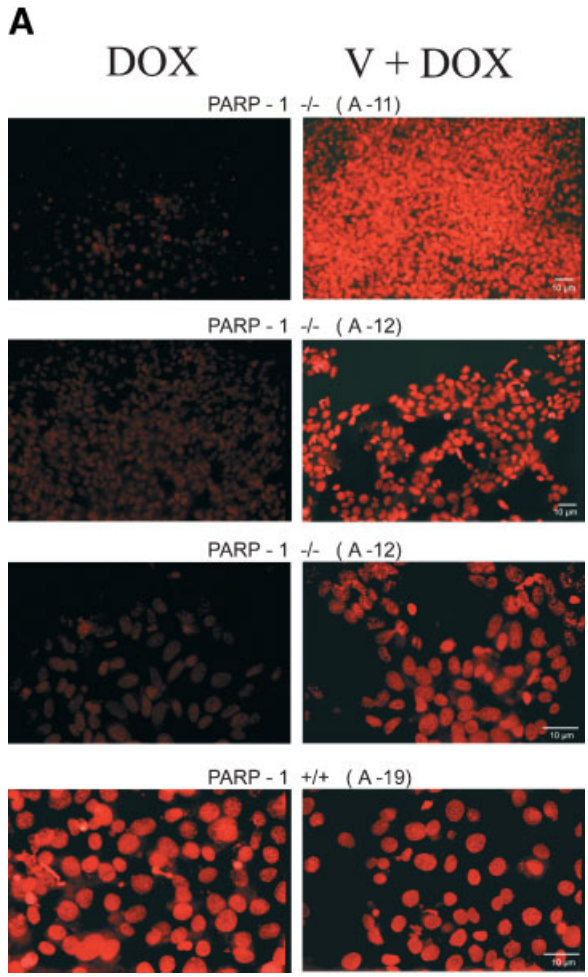

Fig. 1. Enhancement of doxorubicin (DOX) accumulation in poly(ADP-ribose) polymerase-1 (PARP-1) knock-out (KO) mouse cells by multidrug resistance (MDR) modulator. Wild-type (A-19) and PARP-$1^{-/-}$ cells (A-11 and A-12) were exposed to DOX (from 0.05 to 2 μM) for 12 and 24 h. Then cells were fixed with paraformaldehyde (**A**) or detached from substratum and the DOX uptake was measured by FACS (**B**). A: MDR modulator increased DOX accumulation in PARP-1 KO mouse cells. Wild-type (A-19) and PARP-$1^{-/-}$ cells (A-11 and A-12) were exposed to 0.35 μM DOX alone or in combination with 10 μM verapamil (V) for 24 h. Then cells were fixed with paraformaldehyde. The reduced size of PARP-1 KO cells became evident. The images of cells were prepared at a lower magnification (**upper panel**) and at a higher magnification (**lower panel**). B: Quantification of DOX accumulation by FACS. Wild-type (A-19) and PARP-1−/− cells (A-11 and A-12) were exposed to 0.2 μM DOX for 12 h. Then cells were harvested, PBS washed and the fluorescence was measured by FACS. The population of DOX positive cells (R4), shown as blue dots, is indicated by a circle. **C**: Wild-type mouse cells strongly accumulate DOX. A comparison of the frequency of DOX positive cells (R4) among examined cells lines. Mouse cells were exposed for 12 h to increasing concentrations of DOX (0.2–2 μM) alone or in combination with 10 μM verapamil (V). Then cells were harvested, PBS washed and the fluorescence was measured by FACS.

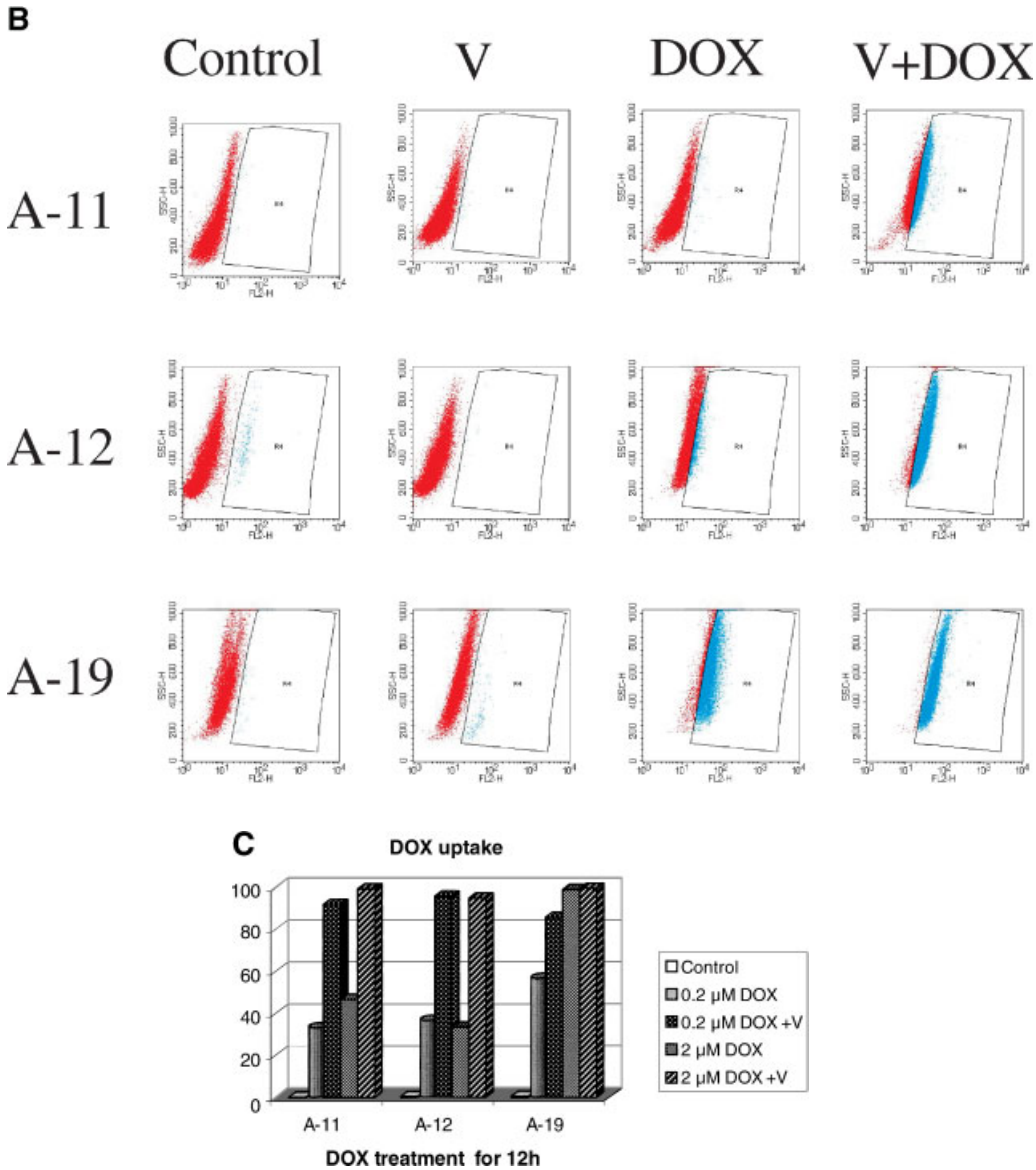

Fig. 1. (*Continued*)

protein band stained in the samples obtained from mouse cells and that of the positive control was comparable. The sequential incubation of the blot with antibodies directed against NF-κB revealed the major signals in the cytosol fraction indicating that NF-κB failed to translocate into the nucleus of PARP-$1^{-/-}$ cells upon the treatment. The lack of induction of stress response after DOX treatment was additionally confirmed by immunoblotting with anti-p53 PAb421 antibodies (Fig. 3B). No p53 signal was detected in mouse samples obtained from DOX-treated cells. After combined treatment with verapamil and DOX at high concentration, p53 protein was induced. However, in the same blot a strong p53 band was detected in the HL-60 sample. This result was surprising for two reasons. First, HL-60 cells cloned from a human promyelocytic leukemia [Dalla-Favera et al., 1982] express neither p53 mRNA nor p53 protein due to major deletions in the *p53* gene [Wolf and Rotter, 1985; Banerjee et al., 1995]. Secondly, the strong p53 reactivity was detected solely with the monoclonal anti-p53 antibody PAb421 but not with human specific DO-1 antibody. The monoclonal anti-p53 PAb421 antibody recognizes wild-type and mutant p53 protein from different species, but its reactivity with p53 protein expressed in human cells is, if any, extremely weak. These observations

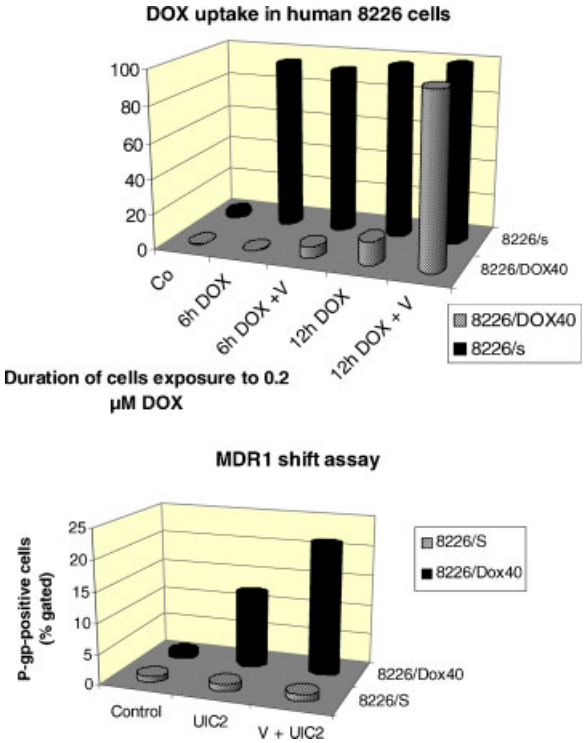

Fig. 2. DOX accumulation and MDR1 shift in 8226/Dox40 cells overexpressing P-gp. [Color figure can be viewed in the online issue, which is available at www.interscience.wiley.com.]

prompted us to repeat the experiments and to compare the P-gp level in mouse cells with that in well-characterized human chemoresistant cell line that overexpress P-gp. We used previously established human myeloma parental 8226/s cells and the cell subclone 8226/Dox40 rendered resistant to DOX during 2-years period [Dalton et al., 1986, 1989]. Immunoblotting analysis of WCLs as well as of the plasma membrane fraction using the monoclonal anti-P-gp antibody C219 revealed the presence of a P-gp band in all three examined mouse cell lines and in the positive control 8226/Dox40. No P-gp band could be detected in a lysate obtained from DOX sensitive human myeloma 8226/s cells, known to be P-glyoprotein negative (Fig. 3C). To quantify the P-gp concentration in distinct mouse cell lines, the intensity of the reactive band at 170 kDa was determined by densitometry. For control, the levels of actin, a chemoresistance unrelated protein, was monitored. The densitometric analysis revealed that PARP-1 deficient mouse cells express about threefold higher amounts of P-gp protein than the normal counterparts. A much higher P-gp expression was detected in lysates prepared from human chemoresistant 8226/Dox40 cell line. Sequential incubation of the blot with the monoclonal anti-p53 antibodies DO-1 or DO-7 revealed a strong p53 band in the latter. This result is in concordance with our previous observation and with published data [Kartner et al., 1985].

In the next step, we proved the reactivity of JSB-1 antibody. We prepared twin blots, the first one was incubated with the monoclonal anti-P-gp C219 antibody and the second one with the commercially available JSB-1 antibody (Fig. 4). To avoid the overstaining of P-gp in the positive control, we used 8226/Dox40 cells cultivated for longer time without DOX and loaded lower protein amounts. The C219 antibody recognized P-gp protein in WCLs prepared from human 8226/Dox40 and from mouse cells (upper panel), whereas the JSB-1 antibody did not stain any band on the twin blot (lower panel). The sequential incubation of the negative blot with the C219 antibody also gave positive P-gp bands thereby indicating that the JSB antibody has a lower affinity to P-gp protein of human origin than C219 antibody and lacks to react with the mouse antigen. This latter observation is consistent with previously published characteristics of the JSB-1 antibody [Scheper et al., 1988]. The sequential incubation of the blots with the anti-p53 antibody PAb421 and then with DO-1 revealed the high expression of p53 protein in human 8226 myeloma cells that was detected solely using the monoclonal anti-p53 antibody DO-1.

Finally, we probed the JSB-1 antibody with blots overloaded with cell lysates from cells overexpressing P-gp. JSB-1 moderately reacted with human antigen. On the basis of these results we assume that a kind gift of the anti-P-gp antibody that we used for incubation of the blot shown in Figure 3A was presumably C219 instead of JSB-1 antibody.

Intracellular Distribution of P-gp Protein

As expected, P-gp protein was detected in the plasma membrane fraction isolated from control and DOX-treated mouse cells (Fig. 5). The levels of plasma membrane associated P-gp proteins varied between wild-type and PARP-1 null cells in a similar way as in WCLs and were much higher in the latter. Furthermore, two other fractions obtained during the isolation of plasma membrane fraction: cytosol yielded

after ultracentrifugation and crude nuclei were additionally submitted to immunoblotting analysis. No P-gp was detected in soluble cytosol, whereas P-gp protein was found in the fraction of crude nuclei. This observation was not surprising for several reasons. First, P-gp protein undergoes post-translational modification steps and for glycosylation it enters the endoplasmic reticulum (ER) [Abbaszadegan et al., 1996]. Since ER is directly connected with the outer nuclear membrane, it is co-precipitated with nuclei during isolation procedure of plasma membrane. Secondly, subcellular fractionation designed for preparation of plasma membrane excludes per se the use of detergents and thereby promotes collapsing of cytoskeletal elements on nuclei [Capco et al., 1982]. Finally, the nuclear immunolocalization of P-gp in multidrug resistant cell lines has been previously described [Baldini et al., 1995]. In the next series of experiments we isolated the nuclei from normal and PARP-1 KO cells according to the procedure described by Capco et al. [1982]. The thorough analysis of P-gp distribution in the subcellular fractions revealed that in the nuclei isolated according to the Penman's procedure, the P-gp amounts were strongly reduced to a barely detectable level (not shown).

Effect of DOX on the Cell-Cycle Progression Differs Between Normal and PARP-1 KO Cells

Finally, to assess the effect of DOX on the cell-cycle we performed the flow cytometric analysis of propidium iodide stained cells. As shown in Figure 6A, the exposure of normal mouse cells to 1 μM DOX for 12 and 24 h induced a strong G_2 block. After 24 h, about 80% of cells were in G_2-phase of the cell-cycle. However, exposure of PARP-1 deficient cells to DOX inhibited primarily the transition between S and G_2 thereby resulting in the accumulation of the cell population remaining in S-phase. DOX reduced significantly the frequency of G_1 cells. The comparison of the G_2/G_1 ratio for each cell line

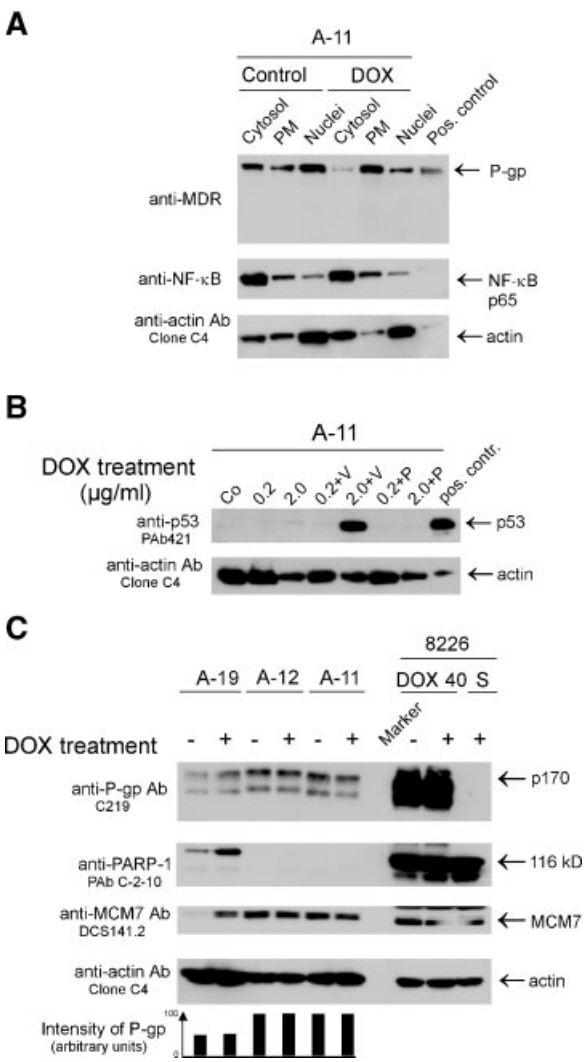

Fig. 3. Increased expression of P-glycoprotein (P-gp) in mouse cells lacking PARP-1. Proteins of whole cell lysates (WCLs) or of distinct subcellular fractions were loaded on 10% (**A** and **B**) or 8% SDS gels and transferred electrophoretically onto PVDF membranes. The efficiency of electrotransfer and of protein loading was proved by Ponceau S staining. A: P-gp expression in PARP-1 KO cells. Subcellular fractions isolated from control and DOX treated PARP-1 KO cells (A-11) were analyzed. The blot was incubated with anti-P-gp antibody at a final dilution of 1:500, and sequentially with anti-NK-κB antibody and anti-actin antibody. A positive control (plasma membrane fraction) obtained from Dr. W. Berger and Dr. E. Elbling was loaded in the last **lane** on the right. B: Induction of p53 protein in PARP-1 KO cells after combined treatment with DOX and verapamil. Samples from untreated control A-11 cells or cells treated for 24 h with DOX alone or in combination with 10 μM verapamil (V) or 1 mg/ml probenecid (P) was resolved on the gel. A positive control (plasma membrane fraction) obtained from Dr. W. Berger and Dr. E. Elbling was loaded in the last **lane** on the right. **C**: Reactivity of P-gp protein with monoclonal C219 antibody. WCLs from control and DOX treated mouse cells were resolved on the gel. WCLs of human 8226/Dox40 and 8226s were loaded as a P-gp-positive and -negative control, respectively. The blot was incubated with the monoclonal anti-P-gp antibody C-219 at a final dilution of 1:1,000. The **lanes**, in which lysates of PARP-1 KO cells were loaded, were unequivocally evidenced after incubation with anti-PARP-1 antibodies. The loading control was performed with anti-actin antibodies. WCLs of wild-type cells were loaded at a slightly higher concentration to detect P-gp. To quantitate the relative amounts of P-gp proteins for each cell line, the autoradiograms were scanned using a densitometer (Bio-Rad Laboratories). The intensity of the P-gp band was then normalized against values of actin and is indicated by black columns.

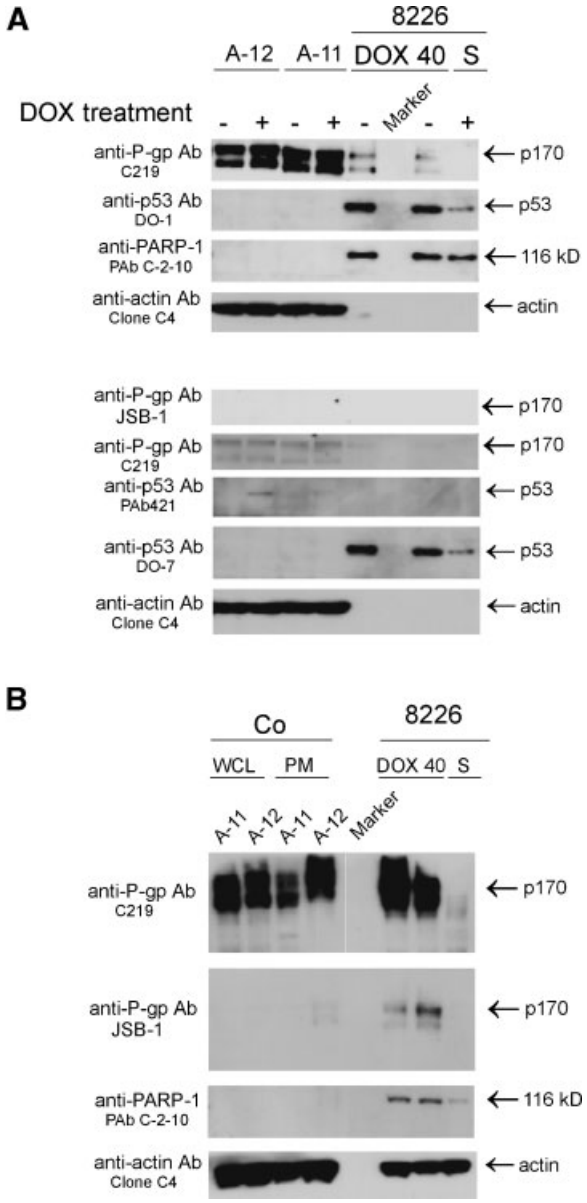

Fig. 4. Differential reactivity of anti-P-gp antibodies with mouse antigens. **A**: WCLs from control and DOX treated mouse (A-12 and A-11) and human (8226) cells were loaded on twin gels. One blot was incubated with monoclonal anti-P-gp C219 antibodies (**upper panel**) at a final dilution of 1:2,000 and the second one with commercially available monoclonal anti-P-gp JSB-1 antibodies 1:1,000 (**lower panel**). The sequential incubation of the blot with C219 antibody generated a high background and therefore only shortly exposed film was suitable for scanning. Sequential incubation with anti-p53 antibodies PAb421 and DO-1 revealed the high expression of p53 protein in 8226 cells that was detectable only by DO-1 or DO-7. **B**: Samples (WCLs or plasma membrane (PM) from control mouse (A-12 and A-11) and human (8226) cells were loaded on twin gels. One blot was incubated with monoclonal anti-P-gp C219 antibodies (**upper panel**) at a final dilution of 1:2,000 and the second one with commercially available monoclonal anti-P-gp JSB-1 antibodies 1:200 (**lower panel**).

(Fig. 6B) revealed a dramatic effect of DOX on the cell-cycle in normal mouse fibroblasts. The combined treatment of cells lacking PARP-1 with verapamil and DOX enhanced the action of DOX (Fig. 6A,C). The inhibition of P-gp by verapamil doubled the DOX-mediated increase G_2 cell population (Fig. 6A). This effect became even more evident at low DOX concentrations (Fig. 6C).

Effect of DOX on the Activity of the Cellular Factors Regulating the Cell-Cycle

The progression of the cell-cycle is primarily regulated by the activity of cyclin–cyclin dependent kinases (CDKs) complexes. Therefore, we examined the phosphorylation status of CDK2 and CDK1 in mouse cells exposed to DOX alone or in combination with verapamil. DOX treatment resulted in a strong activation of site-specific phosphorylation of CDK2 in normal mouse cells but not in PARP-1 mutant cells (Fig. 7). CDK2 was strongly phosphorylated at threonine 160 in WT cells. In contrast, the modification of CDK1 was positively affected in mouse cells by low DOX dose irrespective of their PARP-1 status (Fig. 7). The phosphorylation of threonine 14 and tyrosine 15 increased markedly after 0.2 μM DOX treatment. However, at 10-fold DOX concentration the site specific phosphorylation of CDK1 was obviously reduced in cells lacking PARP-1 (Fig. 7). Moreover, DOX stimulated the site-specific phosphorylation of Myt1, CDK1-related protein kinase. Interestingly, the basal level of phosphorylation of Myt1 at serine Ser83 in unstressed cells differed between cells lacking PARP-1 and their normal counterparts.

Strong Activation of Caspases in PARP-1 KO Cells After Exposure to DOX

Since the DOX treatment more severely affected the proliferation and cell-cycle progression of normal mouse cells, we examined the activity of caspases-3/7, which are essential for the execution of proteolytic cascade during apoptosis. We analyzed separately the enzymatic activity in whole cells and that released into culture medium. DOX at low concentration (0.2 μM) did not significantly activate caspases neither in normal nor in mutant mouse cells (Fig. 8). Interestingly, fivefold higher DOX dose resulted in the activation of caspases-3/7 solely in mouse cells lacking PARP-1. Inhibition of P-gp by verapamil strongly enhanced DOX-

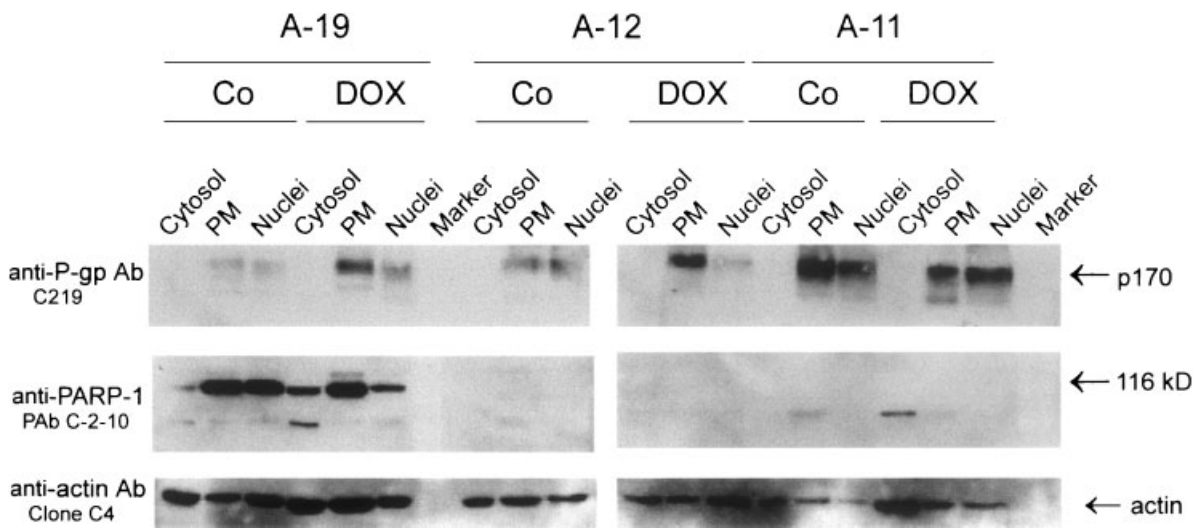

Fig. 5. P-gp protein is primarily anchored in the plasma membrane. Proteins of the subcellular fractions (30 μg of proteins/**lane**) were loaded on gels. Blotting conditions as in Figure 3.

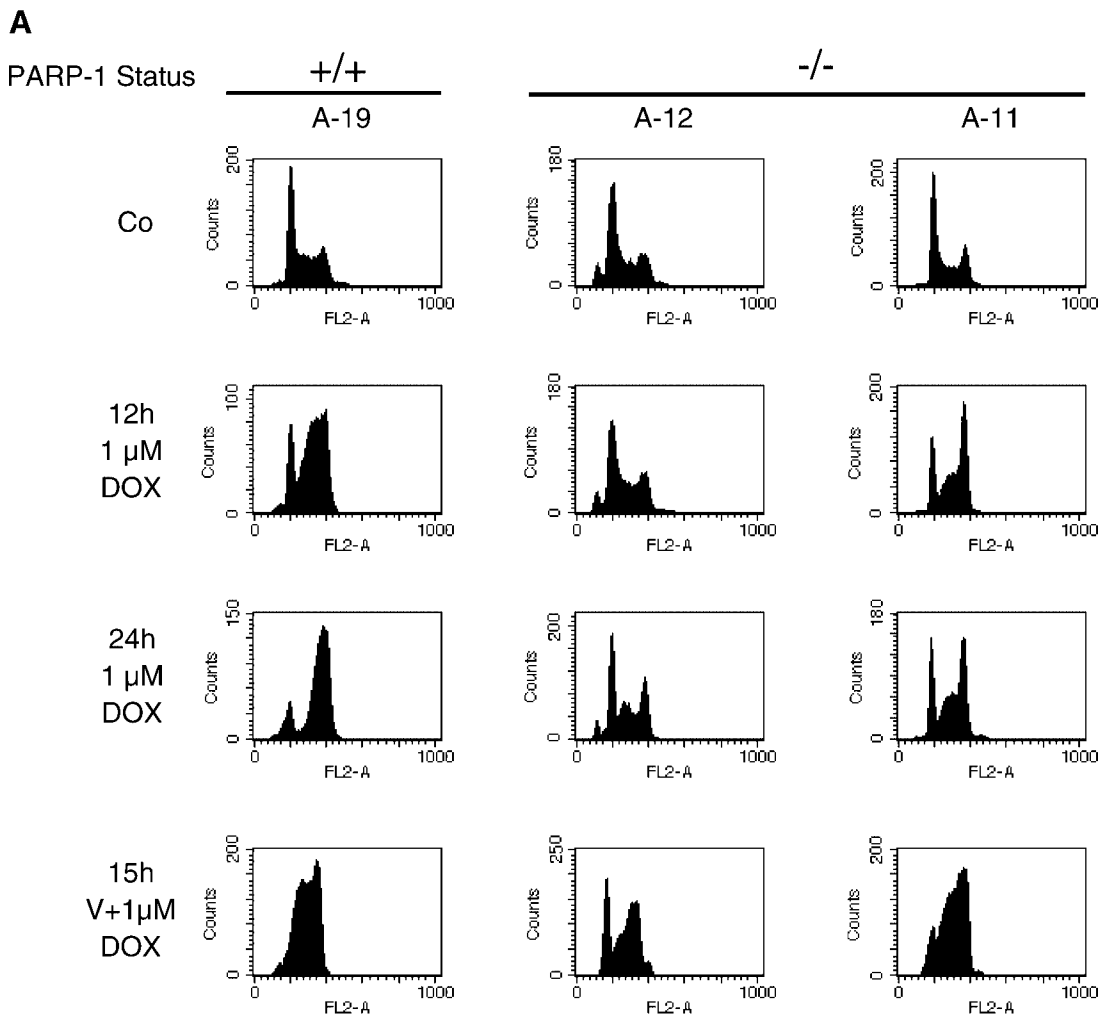

Fig. 6. DOX affects differentially the cell-cycle progression in normal and PARP-1 KO cells. **A**: DOX induces a strong G_2 block in WT MEFs. DNA histograms were obtained by CellQuest evaluation program. **B**: Distribution of mouse cells in distinct cell-cycle phases. Distribution of cells in distinct cell-cycle phases was determined using ModFIT cell-cycle analysis software. **C**: DOX-induced G_2 block is accompanied by reduction of G_1 population in normal mouse cells. **D**: Inhibition of P-gp in PARP-1 KO cells exposed to DOX results in a G_2 block. DNA histograms were obtained by CellQuest evaluation program. [Color figure can be viewed in the online issue, which is available at www.interscience.wiley.com.]

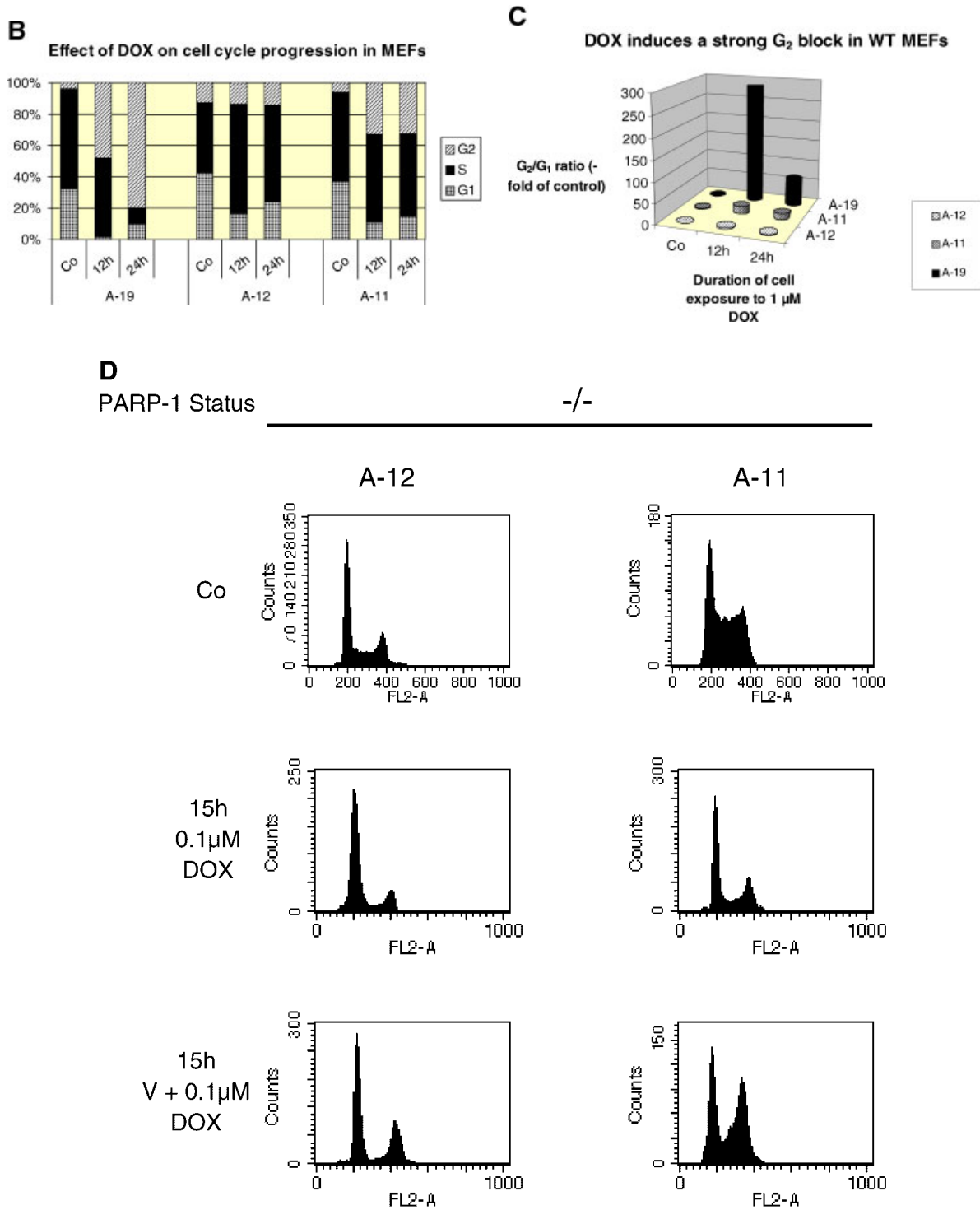

Fig. 6. (*Continued*)

mediated activation of caspases (Fig. 8) indicating that the extent of caspases 3/7 activation in cells lacking PARP-1 correlates with the intracellular accumulation of the drug. The analysis of culture medium revealed the release of activated caspase-3/7 after exposure of PARP-1 KO cells to 1 μM DOX that was essentially augmented after inhibition of P-gp activity (not shown). These results correlate closely with the apoptotic changes observed in whole cells.

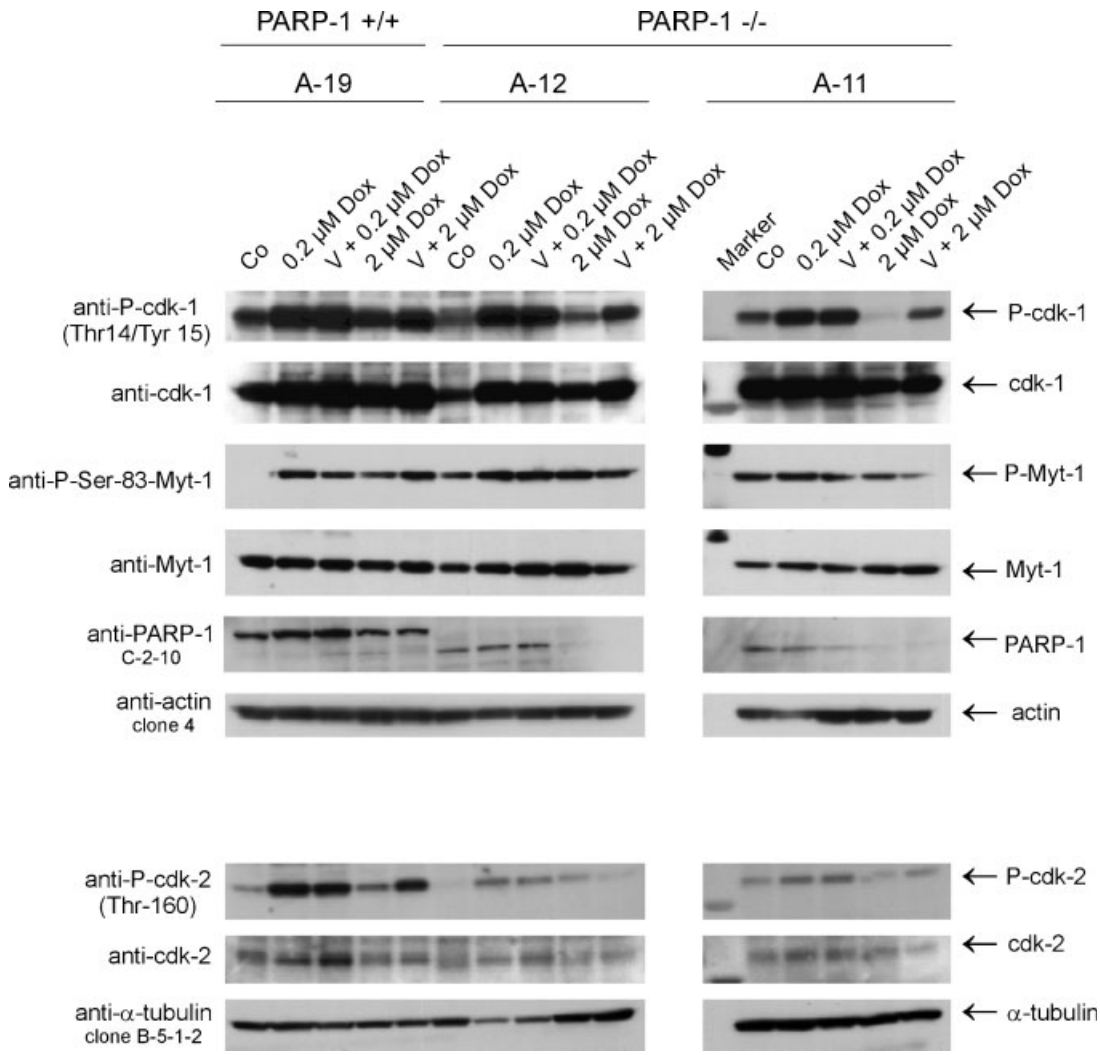

Fig. 7. Effect of DOX treatment on the activity status of factors regulating cell-cycle. WCL obtained from untreated control cells and cells treated for 24 h with DOX alone or in combination with verapamil (V) were resolved on 12% SDS gels. The phosphorylation status of CDK1 and CDK2 was examined using antibodies recognizing site-specific phosphorylation of the corresponding CDKs. To visualize the total level of the corresponding CDKs, the blots were sequentially incubated with antibodies, which recognize proteins irrespective their phosphorylation state. The equal protein loading and transfer was confirmed by Ponceau S staining and additionally evidenced by examination of cellular level of actin using a monoclonal anti-actin antibody (Clone 4 from ICN) or by examination of cellular level of α-tubulin using monoclonal anti-α-tubulin antibody (Clone B-5-1-2 from Sigma).

DISCUSSION

One reason for the failure of many chemotherapeutic protocols in the treatment of human cancers is the development of resistance against a wide range of anti-cancer drugs. Determining mechanisms of drug resistance and developing tools for identifying drug resistant cells could provide the basis for advances in the improvement of therapeutic settings. One type of resistance that is termed multiple-drug resistance was observed frequently in tumor cells. The cancer cells develop a resistance to a number of drugs that are heterogeneous in structure and action. Tumor cells exhibiting MDR phenotype frequently overexpress a 170 kDa membrane glycoprotein P-gp. To establish a model system for identifying mechanisms of resistance to anti-cancer drugs, cell lines were cultivated for a long time in the presence of increasing concentrations of anti-cancer drugs such as DOX or vinblastin. By selection one can develop a population of cells that is enriched in highly resistant cells by killing the sensitive cells and allowing the resistant cells to multiply. A consequence of this strategy is elevation of the

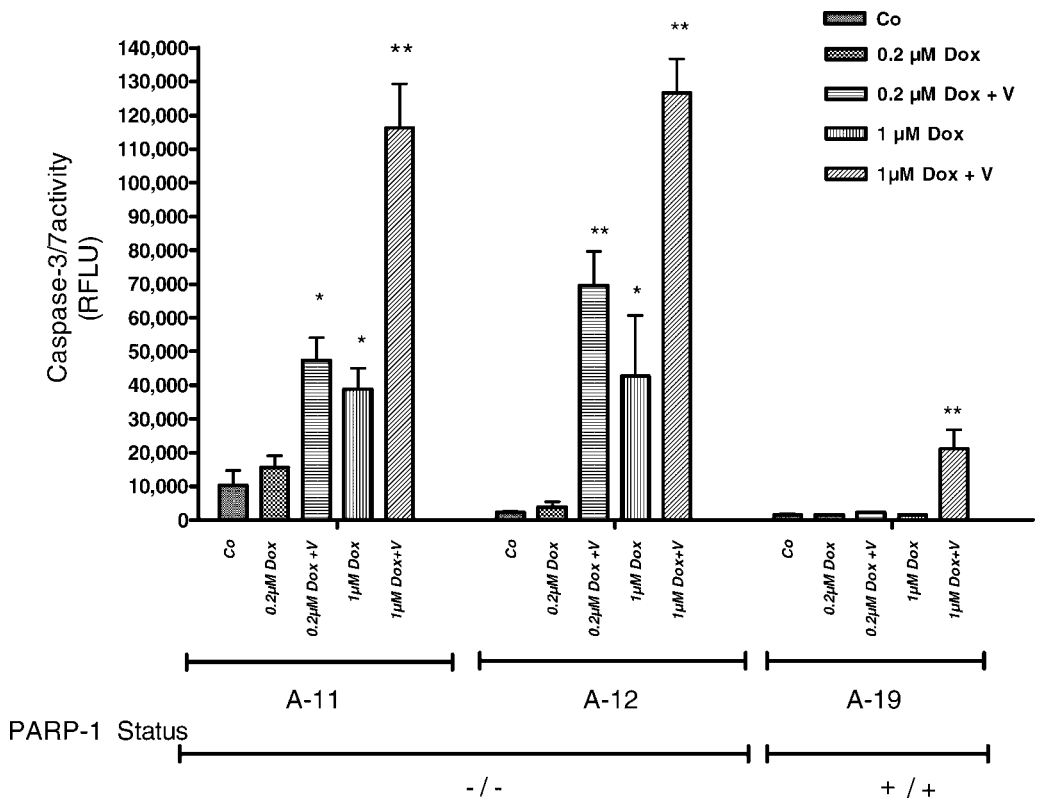

Fig. 8. A strong activation of caspase-3/7 in PARP-1 deficient cells at high DOX concentration. Caspase 3/7 activity was determined quantitatively using APO-ONE Caspase 3/7 Assay (Promega). Cells were mixed with caspases substrate Z-DEVD-R110. After 4 h incubation at 37°C, fluorescence was measured at 485 nm. Culture medium was used as a blank. Three replicates of each sample were measured. Assay was repeated four times. Statistical significance was determined using the ANOVA test followed by Dunnett's Multiple Comparison test (all treatment groups vs. corresponding control). Bars indicate means ± SD. Asterisks indicate statistical significance valuated with ANOVA test: $^{**}P < 0.01$, $^{*}P < 0.05$.

expression of drug efflux pumps or metabolizing enzymes and alteration in expression of genes encoding the targets of drug action. Analysis of the changes of gene expression that accounted for the resistance allowed to identify the genes encoding the efflux pump P-gp [Juliano and Ling, 1976; Chen et al., 1986], the MRP1 [Cole et al., 1992], and ABCP [Doyle et al., 1998; Miyake et al., 1999]. P-gp, a 170 kDa integral membrane protein, belongs to the superfamily of structurally related ABC (ATP-binding cassette) membrane transporters that bind covalently to ATP [Gottesman, 1993]. Sequence analysis revealed that P-gp, consisting of 1,280 amino acids, possesses 12 transmembrane domains with 6 transmembrane loops in 2 homologous halves. P-gp is post-translationally modified, the glycosylation by mannose moieties is a major modification. The covalently N-linked multiple carbohydrate residues resulting in the shift of the molecular weight contribute to the size heterogeneity of P-gp.

P-gp is expressed in a several cell types in normal tissues. It has been detected in epithelial cells of the liver, large intestine, and kidney. P-gp was also found in mouse embryonic fibroblast lines NIH/3T3. Brain microvascular endothelial cells express P-gp, which contributes to the blood–brain barrier. The physiological function of P-gp in normal tissues is not fully understood. One can speculate that P-gp is involved in transepithelial transport of xenobiotics and toxic metabolites and may essentially contribute to the barrier function. P-gp protein seems to be also involved in the regulation of chloride channel activity.

We observed previously that the efficacy of some anti-cancer drugs such as DOX or C-1305 in MEFs depends on the functional status of PARP-1 [Wurzer et al., 2000; Lövborg et al., 2002; Wesierska-Gadek et al., 2004]. A number of anti-cancer agents target cellular DNA resulting in its damage and finally the generation of DNA strand breaks. Considering the fact

that PARP-1 is a very potent sensor of DNA strand breaks, it is not surprising that susceptibility of cells to distinct drugs and cellular outcomes after chemotherapy may be related to the cellular status of PARP-1. DOX, a drug frequently used in the cancer therapy intercalates into the DNA helix and generates DNA strand breakage by inhibition of topoisomerase II and by oxidative stress.

Remarkably, DOX induced within a few hours a strong p53 response in normal but not in PARP-1 KO cells. After prolonged exposure of the latter to the combined treatment with verapamil and high DOX concentration, p53 protein was upregulated [Wurzer et al., 2000]. The comparative analysis of the P-gp levels in wt mouse cells and cells lacking PARP-1 revealed enhanced expression of P-gp in the latter [Wurzer et al., 2000]. To ensure that the decreased susceptibility of PARP-1 KO cells to DOX is attributable to MDR phenotype, we performed a new series of experiments in which paralelly to MEFs, the human sensitive and drug resistant cells were included. We observed that the phenotype of PARP-1 KO cells resembled that of human resistant 8226/Dox40 cells. Both cell types accumulated DOX only at low levels and the MDR reversor, verapamil, strongly increased the DOX uptake. Immunoblotting experiments performed with the monoclonal anti-P-gp C219 antibody confirmed the elevated expression of P-gp in PARP-1 deficient cells. The densitometric quantification of the p170 band revealed about threefold higher P-gp expression in mutant cells as compared with the normal counterparts. Remarkably, inspection of the autoradiograms after short exposure revealed that the monoclonal anti-P-gp C219 antibody reacted in samples obtained from MEFs and in human 8226/Dox40 cells with a double band at 170/180 kDa. The P-gp doublet appeared in lanes in which WCLs were loaded. This observation is consistent with features of P-gp. p170 is a glycoprotein and is modified at multiple sites by N-linked mannose moieties. The post-translational modification occurring in ER results in a shift of the protein band. It has been previously evidenced [Dalton et al., 1989] that the monoclonal anti-P-gp C219 antibody recognizes P-gp irrespective of the modification. Two closely related bands at about 170 kDa detected in WCLs represent the nascent and modified protein. It is not surprising that both forms: de novo translated and mature P-gp protein are present in total cell lysates. On the other hand, one could expect that in the plasma membrane primarily the mature P-gp form is anchored.

Moreover, the functionality of the P-gp in our reference cell line 8226/Dox40 was additionally checked by MDR1 shift assay. The principle of the assay is based on the capability of the monoclonal anti-P-gp UlC2 antibody to detect active MDR1. UlC2 inhibits the activity of P-gp and preferentially recognizes P-gp that is in the process of transporting substrates. The monoclonal UlC2 antibody appears to preferentially bind to MDR1 that has completed its catalytic cycle and hydrolyzed ATP. Pretreatment of 8226/Dox40 cells with vinblastine increased the binding of the monoclonal UlC2 antibody.

The analysis of the effect of DOX action on the cell-cycle progression revealed the differential susceptibility of wt and PARP-1 KO cells to the drug. DOX reduced significantly the frequency of G_1 cells and arrested very rapidly the normal MEFs in G_2-phase of the cell-cycle. In contrast, PARP-1 deficient cells were inhibited by DOX primarily in the transition between S and G_2 thereby resulting in the accumulation of the cell population residing in S-phase. However, the combined treatment with MDR reversor arrested the mutant cells in G_2-phase. Thus, the inhibition of P-gp activity resulting in the elevation of intracellular DOX concentration blocked PARP-1 deficient cells in G_2. These results implicate that the differential effect of DOX on the distribution of mouse cells in distinct phases of the cell-cycle does not depend on PARP-1 status but is rather related to the intracellular level of DOX. Interestingly, differences in the DNA profiles after DOX treatment were reflected by differential activity of essential components regulating the cell-cycle. Most striking difference was observed in the action of DOX on the functional status of CDK2. CDK2 activity is essential for entry into the S-phase of the cell-cycle [Nurse, 1997; Helin, 1998; Nurse et al., 1998]. Activated CDK2 in complexes with cyclin E and cyclin A is assumed to phosphorylate proteins whose activity is directly implicated in regulating the initiation of DNA replication [Nurse, 1997; Nurse et al., 1998]. The activation of CDK2 is caused by its phosphorylation at threonine 160. Remarkably, the exposure of mouse cells to low DOX concentrations induced site-specific phosphorylation of CDK2 in normal but not in mutant cells thereby

explaining the basis of the accumulation of the latter in the S-phase. On the other hand, the DOX-mediated block at the G_2-M border was attributable to the maintenance of CDK1 complexes in the inactive state in DOX-treated cells. Progression through G_2- and M-phase is regulated by CDK1 in association with cyclin A and cyclin B [Nurse, 1997; Nurse et al., 1998]. The phosphorylation of CDK1 at Thr14, Tyr15, and finally at Thr161 is necessary for initial activation of the CDK1/cyclin complexes. The site specific-phosphorylation of distinct residues of CDK1 is catalyzed by specific protein kinases: Myt1 and Wee1 [Nurse, 1997; Nurse et al., 1998]. However, the onset of mitosis is regulated by sequential dephosphorylation of CDK1 at Thr14 and Tyr15. Activatory Cdc25C protein phosphatase is responsible for determining the phosphorylation state of CDK1, which only achieves full protein kinase activity when Thr14/Tyr15 are dephosphorylated. The induction of phosphorylation of Myt1 at serine 83 observed primarily in DOX treated normal mouse cells coincides with the increase of the modification of Thr14/Tyr15 of CDK1. The activity of Myt1, the protein kinase responsible for the phosphorylation of CDK1 at Thr 14 is also regulated by modification. Myt1 upon phosphorylation at serine 83 is capable of phosphorylation of CDK1 at threonine 14.

Moreover, we observed that DOX activated strongly caspase-3/7 in PARP-1 deficient cells. The extent of caspases activation correlated directly with the cellular accumulation of DOX. Higher DOX dose and suppression of P-gp potentiated the activation of caspases and resulted their release into the culture medium. These observations indicate that DOX at high concentrations initiate apoptosis in mouse fibroblasts and that the inactivation of PARP-1 promotes the induction of apoptotic changes.

Taking together our results evidence that mouse cells lacking functional PARP-1 express higher levels of P-gp, which correlates with the MDR phenotype. What could be a reason of the P-gp upregulation in PARP-1 deficient mouse cells? The expression of P-gp protein is known to be negatively regulated by wt p53 tumor suppressor protein [Chin et al., 1992; Wang and Beck, 1998]. The strong reduction of the basal level of wt p53 after disruption of *PARP-1* gene [Wesierska-Gadek et al., 1999] could be responsible for the loss of the negative regulation of P-gp and could contribute to the development of MDR phenotype. Recently, resistance of 53 KO cells to DOX was described [Dunkers et al., 2003]. The observed resistance to DOX was related to decreased formation of DNA strand breaks in the absence of functional p53. On the other hand, it has been proposed that aneuplopid cell lines can acquire resistance against multiple drugs by chromosome reassortments catalyzed by aneuploidy [Duesberg et al., 2001]. Inactivation of PARP-1 by gene disruption in mouse [Wang et al., 1995] cells led to a number of genetic alterations and chromosomal abnormalities [d'Adda di Fagagna et al., 1999; Simbulan-Rosenthal et al., 2000]. Cytogenetic analysis of mouse embryonic fibroblasts revealed that the disruption of the gene encoding PARP-1 is associated with severe chromosomal instability, characterized by increased frequencies of chromosome fusions and aneuploidy [d'Adda di Fagagna et al., 1999]. Moreover, PARP-1 null mice exhibit an unstable tetraploid population, and partial chromosomal gains and losses [Simbulan-Rosenthal et al., 2000]. Oligonucleotide microarray analysis applied to characterize more comprehensively the differences in gene expression between asynchronously dividing primary fibroblasts derived from PARP-1 null mice and their wild-type littermates revealed that of the 11,000 genes monitored, 91 were differentially expressed in mutant mice [Simbulan-Rosenthal et al., 2000]. Immortalized PARP-1 deficient fibroblasts are accompanied by changes in the expression of p53, Rb, and c-Jun, as well as other proteins [Simbulan-Rosenthal et al., 2000].

Considering the fact that disruption of *PARP-1* gene results in the genetic instability and aneuploidy, we cannot exclude that the chromosome reassortments could also be responsible for the acquisition of spontaneous drug resistance.

ACKNOWLEDGMENTS

I thank Ms. M. Eisenbauer and Ms. A. Maderner for cultivation of cells, Mr. P. Breit for preparation of photomicrographs and Dr. J. Wojciechowski for preparation of graphics.

REFERENCES

Abbaszadegan MR, Cress AE, Futscher BW, Bellamy WT, Dalton WS. 1996. Evidence for cytoplasmic P-glycoprotein location associated with increased multidrug resistance and resistance to chemosensitizers. Cancer Res 56: 5435–5442.

Ame JC, Spenlehauer C, de Murcia G. 2004. The PARP superfamily. Bioessays 26:882–893.

Baldini N, Scotlandi K, Serra M, Shikita T, Zini N, Ognibene A, Santi S, Ferracini R, Maraldi NM. 1995. Nuclear immunolocalization of P-glycoprotein in multidrug-resistant cell lines showing similar mechanism of doxorubicin distribution. Eur J Cell Biol 68:226–239.

Banerjee D, Lenz HJ, Schnieders B, Manno DJ, Ju JF, Spears CP, Hochhauser D, Danenberg K, Bertino JR. 1995. Transfections of wild-type but not mutant p53 induces early monocytic differentiation in HL-60 cells and increases their sensitivity to stress. Cell Growth Differ 6:1405–1413.

Calabrese CR, Almassy R, Barton S, Batey MA, et al. 2004. Anticancer chemosensitization and radiosensitization by the novel poly(ADP-ribose) polymerase-1 inhibitor AG14361. J Natl Cancer Inst 96:56–67.

Capco DG, Wan KM, Penman S. 1982. The nuclera matrix: Three dimensional architecture and protein composition. Cell 29:847–858.

Chatterjee S, Cheng MF, Berger RB, Berger SJ, Berger NA. 1995. Effect of inhibitors of poly(ADP-ribose) polymerase on the induction of GRP78 and subsequent development of resistance to etoposide. Cancer Res 55:868–873.

Chen CJ, Chin JE, Ueda K, Clark DP, Pastan I, Gottesman MM, Roninson IB. 1986. Internal duplication and homology with bacterial transport proteins in the mdr1 (P-glycoprotein) gene from multidrug-resistant human cells. Cell 47:381–389.

Chin KV, Ueda K, Pastan I, Gottesman MM. 1992. Modulation of activity of the promoter of the human *MDR1* gene by Ras and p53. Science 255:459–462.

Cole SP, Bhardwaj G, Gerlach JH, Mackie JE, Grant CE, Almquist KC, Stewart AJ, Kurz EU, Duncan AM, Deeley RG. 1992. Overexpression of a transporter gene in a multidrug-resistant human lung cancer cell line. Science 258:1650–1654.

d'Adda di Fagagna F, Hande MP, Tong WM, Lansdorp PM, Wang ZQ, Jackson SP. 1999. Functions of poly(ADP-ribose) polymerase in controlling telomere length and chromosomal stability. Nat Genet 23:76–80.

D'Amours D, Desnoyers S, D'Silvia I, Poirier GG. 1999. Poly(ADP-ribosyl)ation reactions in the regulations of nuclear functions. Biochem J 342:249–268.

Dalla-Favera R, Wong-Staal F, Gallo RC. 1982. Onc gene amplification in promyelocytic leukemia cell line HL-60 and primary leukaemic cells of the same patient. Nature 299:61–63.

Dalton WS, Durie BG, Alberts DS, Gerlach JH, Cress AE. 1986. Characterization of a new drug-resistant human myeloma cell line that expresses P-glycoprotein. Cancer Res 46:5125–5130.

Dalton WS, Grogan TM, Rybski JA, Scheper RJ, Richter L, Kailey J, Broxterman HJ, Pinedo HM, Salmon SE. 1989. Immunohistochemical detection and quantification of P-glycoprotein in multiple drug-resistant human myeloma cells: Association with level of drug-resistance and drug accumulation. Blood 73:747–752.

Delaney CA, Wang LZ, Kyle S, White AW, Calvert AH, Curtin NJ, Durkacz BW, Hostomsky Z, Newell DR. 2000. Potentiation of temozolomide and topotecan growth inhibition and cytotoxicity by novel poly(adenosine diphosphoribose) polymerase inhibitors in a panel of human tumor lines. Clin Cancer Res 6:2860–2867.

Doyle LA, Yang W, Abruzzo LV, Krogmann T, Gao Y, Rishi AK, Ross DD. 1998. A multidrug resistance transporter from human MCF-7 breast cancer cells. Proc Natl Acad Sci USA 95:15665–15670.

Duesberg P, Stindl R, Hehlmann R. 2001. Origin of multidrug resistance in cells with and without multidrug resistance genes: Chrmosome reassortments catalyzed by aneuploidy. Proc Natl Acad Sci USA 98: 11283–11288.

Dunkers TR, Wedemeyer I, Baumgartner M, Fritz G, Kaina B. 2003. Resistance of p53 knockout cells to doxorubicin is related to reduced formation of DANN strand breaks rather that impaired apoptotic signaling. DNA Repair-(Amst) 2:49–60.

Gottesman MM. 1993. How cancer cells evade chemotherapy: Sixteenth Richard and Hinda Rosenthal Foundation Award lecture. Cancer Res 53:747–754.

Helin K. 1998. Regulation of cell proliferation by the E2F transcription factors. Curr Opin Genet Dev 8:28–35.

Juliano RL, Ling V. 1976. A surface glycoprotein modulating the drug permeability in Chinese hamster ovary cell mutants. Biochim Biophys Acta 455:152–162.

Kartner N, Evernden-Porelle D, Bradly G, Ling V. 1985. Detection of P-glycoprotein in multidrug-resistant cell lines by monoclonal antibodies. Nature 316:820–823.

Lemke K, Poidessous V, Skladanowski A, Larsen AK. 2004. The antitumor triazoloacridone C-1305 is a topoisomerase II poison with unusual properties. Mol Pharmacol 66:1035–1042.

Lövborg H, Wojciechowski J, Larsson R, Wesierska-Gadek J. 2002. Action of a novel anticancer agent, CHS 828, on mouse fibroblasts: Increased sensitivity of cells lacking poly(ADP-ribose) polymerase-1. Cancer Res 62:4206–4211.

Miyake K, Mickley L, Litman T, Zhan Z, Robey R, Cristensen B, Brangi M, Greenberger L, Dean M, Fojo T, Bates SE. 1999. Molecular cloning of cDNA which are highly overexpressed in mitoxantrone-resistant cells: Demonstration of homology to *ABC* transport genes. Cancer Res 59:8–13.

Nurse P. 1997. Regulation of the eukaryotic cell cycle. Eur J Cancer 33:1002–1004.

Nurse P, Masui Y, Hartwell L. 1998. Understanding the cell cycle. Nat Med 4:1103–1106.

Riordan JR, Ling V. 1979. Purification of P-glycoprotein from plasma membrane vesicles of Chinsese hamster ovary cell mutants with reduced colchicines permeability. J Biol Chem 254:12701–12705.

Scheper RJ, Bulte JW, Brakkee JG, Quak JJ, van der Schoot E, Balm AJ, et al. 1988. Monoclonal antibody JSB-1 detects a highly conserved epitope on the P-glycoprotein associated with multi-drug resistance. Int J Cancer 42:389–394.

Simbulan-Rosenthal CM, Ly DH, Rosenthal DS, Konopka G, Luo R, Wang ZQ, Schultz PG, Smulson ME. 2000. Misregulation of gene expression in primary fibroblasts lacking poly(ADP-ribose) polymerase. Proc Natl Acad Sci USA 97:11274–11279.

Szabo C, Dawson VL. 1998. Role of poly(ADP-ribose) synthetase in inflammation and ischaemia-reperfusion. Trends Pharmacol Sci 19:287–298.

Vindelov LL, Christensen IJ, Keiding N, Spang-Thomsen M, Nissen NI. 1983. Long-term storage of samples for flow cytometric DNA analysis. Cytometry 3:317–322.

Wang Q, Beck WT. 1998. Transcriptional suppression of multidrug resistance-associated protein (MRP) gene expression by wild-type p53. Cancer Res 58:5762–5769.

Wang ZQ, Auer B, Stingl L, Berghammer H, Haidacher D, Schweiger M, Wagner FF. 1995. Mice lacking ADPRT and poly(ADP-ribosyl)ation develop normally but are susceptible to skin disease. Genes Dev 9:509–520.

Wesierska-Gadek J., Schmid G. 2000. Overexpressed poly(ADP-ribose) polymerase delays the release of rat cells from p53-mediated G1 checkpoint. J Cell Biochem 80:85–103.

Wesierska-Gadek J, Wang ZQ, Schmid G. 1999. Reduced stability of regularly spliced but not alternatively spliced p53 protein in PARP-deficient mouse fibroblasts. Cancer Res 59:28–34.

Wesierska-Gadek J, Schloffer D, Kotala V, Horky M. 2002. Escape of p53 protein from E-6 mediated degradation of HeLa cells after cisplatin therapy. Int J Cancer 101: 128–136.

Wesierska-Gadek J, Schloffer D, Gueorguieva M, Uhl M, Skladanowski A. 2004. Increased susceptibility of poly-(ADP-ribose) polymerase-1 knockout cells to antitumor triazoloacridone C-1305 is associated with permanent G_2 cell cycle arrest. Cancer Res 64:4487–4497.

Wojciechowski J, Horky M, Gueorguieva M, Wesierska-Gadek J. 2003. Rapid onset of nucleolar disintegration preceding cell cycle arrest in roscovitine-induced apoptosis of human MCF-7 breast cancer cells. Int J Cancer 106:486–495.

Wolf D, Rotter V. 1985. Major deletions in the gene encoding the p53 tumor antigen cause lack of p53 expression in HL-60 cells. Proc Natl Acad Sci USA 82:790–794.

Wurzer G, Herceg Z, Wesierska-Gadek J. 2000. Increased resistance to anticancer therapy of mouse cells lacking the poly(ADP-ribose) polymerase attributable to up-regulation of the multidrug resistance gene product P-glycoprotein. Cancer Res 60:4238–4244.